processes

MDPI

Article

Influence of Particle Properties on Filter Cake Compaction Behavior under Oscillatory Shear

Tolga Yildiz *, Joel Gegenheimer, Marco Gleiß and Hermann Nirschl

Institute of Mechanical Process Engineering and Mechanics (MVM), Karlsruhe Institute of Technology (KIT), Straße am Forum 8, 76137 Karlsruhe, Germany; uquox@student.kit.edu (J.G.); marco.gleiss@kit.edu (M.G.); hermann.nirschl@kit.edu (H.N.)

* Correspondence: tolga.yildiz@kit.edu

Abstract: Filter cake compaction is a common method for mechanical deliquoring of compressible filter cakes. In addition to the conventional squeezing compaction method, applying oscillatory shear to filter cakes at low pressure is an alternative compaction process in cake filtration. While basic differences in terms of compaction success have already been identified for various materials, a systematic analysis of the influence of material properties on compaction behavior under oscillatory shear is missing. The present work addresses the influence of particle size distribution and increasing particle agglomeration on the compaction success of oscillatory shear to further clarify the process knowledge and applicability. The compressibility achieved by this technique was investigated for calcium carbonate materials with various particle size distributions. The results show that the compaction potential increases from 17.3% for the coarsest material ($x_{50,3}$ = 23.5 µm) to 26.6% for the finest material ($x_{50,3}$ = 2.3 µm) with decreasing mean particle size. The more widely distributed material exhibits a higher compaction potential of 21.7% compared to 18.4% for the narrowly distributed material. Increasing particle agglomeration to improve the slurry filterability does not affect the achievable compaction states of the material by vibration compaction at sufficiently high energy input.

Keywords: cake filtration; mechanical deliquoring; compressible filter cakes; vibration; compaction; particle size distribution

Citation: Yildiz, T.; Gegenheimer, J.; Gleiß, M.; Nirschl, H. Influence of Particle Properties on Filter Cake Compaction Behavior under Oscillatory Shear. *Processes* **2023**, *11*, 2076. https://doi.org/10.3390/pr11072076

Academic Editor: Alberto Di Renzo

Received: 19 May 2023
Revised: 3 July 2023
Accepted: 8 July 2023
Published: 12 July 2023

1. Introduction

For the separation of solid particles dispersed in high concentration in a liquid phase, cake filtration is a suitable process. By applying a pressure difference, the liquid flows through a filter medium while the particles form a porous filter cake on the filter medium. Further liquid can be removed from the pore volume of the fully saturated filter either mechanically or thermally [1–3]. Although complete mechanical deliquoring is not possible, mechanical processes are more energy-saving and economical than thermal drying [2]. Therefore, it is necessary to deliquor the filter cake mechanically as much as possible before removing the remaining liquid by thermal drying [4].

The application of a gas pressure difference to the filter cake is a mechanical method that leads to a displacement of liquid from the pores and, thus, to cake desaturation. For significant desaturation, the capillary entry pressure must be exceeded by the gas pressure difference. The size of the capillary entry pressure depends not only on the surface tension and the contact angle between the particles and liquid but also on particle properties such as the particle size distribution [5]. For fine, compressible filter cakes, the application of a gas pressure difference induces filter cake shrinkage, which can lead to the formation of filter cake cracks [6–8]. Shrinkage cracks increase the gas throughput and, thus, the operating costs. Slurry properties such as the slurry concentration [9] or operating parameters such as the compressive pressure [10–12] and the cake height [8] affect the shrinkage and cracking potential. Furthermore, particle properties have a decisive impact on the formation of

shrinkage cracks. Wiedemann [12] found that cake shrinkage begins below a mean particle size of 20–50 µm and increases with decreasing mean particle size and width of particle size distribution.

For fine-particulate, compressible filter cakes exhibiting a porosity gradient after cake formation, compaction by squeezing is also a common method for mechanical cake deliquoring. Cake compaction further displaces liquid from the cake by reducing the pore volume. Compaction by squeezing for deliquoring of fine, compressible filter cakes is already utilized in industrial filter apparatuses such as filter presses, membrane filter presses, and belt filter presses [3,13]. Furthermore, cake compaction prior to desaturation by a gas pressure difference is used to avoid shrinkage cracks [12,14,15]. The compaction potential of filter cakes by squeezing is mainly driven by particle properties such as particle size distribution and particle shape. According to Tiller and Yeh [16], filter cakes with a high porosity, in particular, exhibit significant compactibility by squeezing. Highly porous filter cakes are formed mainly by particles with a mean particle size below 10–20 µm, as interparticle forces become larger than mass forces. Wakeman et al. [17] stated that particles larger than 20 µm are nearly incompressible. Furthermore, particles with an irregular shape form more porous structures than regularly shaped particles [16]. For example, plate-like particles produce an open house-of-cards structure that is converted to a roof-tile-like, highly compacted structure by squeezing [18]. The causes of filter cake compaction by squeezing are particle rearrangement processes resulting from the destruction of particle bridges, movement of fine particles in void volumes, and elastic–plastic particle deformation due to external stress [19–23].

However, a challenge of compaction by squeezing is that the required compressive pressure to avoid cracking [12] and significant deliquoring [23] can be very high, depending on the material. If compaction by squeezing is implemented on a drum or belt filter, preferably used due to their continuous operation, an extra design of the mechanical apparatus components may be necessary, resulting in higher costs due to the immense stress caused by the high compressive pressures. Therefore, alternative approaches for additional cake deliquoring are required. An alternative compaction method is the use of steady shear at lower pressures. The effect of shear is already used in belt filter presses to improve the dewatering of highly compressible materials in wastewater treatment [24,25] or juice extraction [26,27]. The benefit of steady shear for filter cake deliquoring also depends, in this case, on the nature of the slurry. In lab-scale press shear cells, several authors have observed positive effects of shear for cake deliqouring to various degrees of kaolin [28,29], mica [28], talc [29], titanium dioxide [30], and limestone [31,32]. However, for activated sludge, as a highly compressible material, Vaxelaire [29] showed that shear did not contribute to any additional deliquoring due to the high cake resistance and the lack of rigidity of the particles for rearrangement. The mechanical deliqouring of coal filter cakes on a vacuum belt filter can be enhanced by an add-on flapper roller according to Bickert and Vince [33]. High Pressure Dewatering Rolls, a continuous filtration apparatus developed by Höfgen et al. [34], achieved a significant improvement in mechanical deliquoring for fibers and alum sludge compared to conventional separation apparatuses by combining shear and compression. For algae, calcium carbonate, and paper mill wastewater, deliquoring results comparable to those of industrial applications can be realized by the apparatus.

Another approach for cake compaction is the use of oscillatory shear, which is already being applied as a conventional method to compact soils [35], granular materials [36], and powders [37]. In microfiltration, it is also established that oscillatory shear at the membrane–fluid interface generated by an oscillatory membrane reduces fouling and, thus, improves the filtration performance [38,39]. In the field of cake filtration, the application of vibrations perpendicular to the filter cake surface for cake deliquoring is already known. Pearce [40] investigated this technique for a membrane filter press and a vacuum filter to improve the deliquoring of China clay, magnesium oxide, calcium carbonate, coal, and titanium dioxide filter cakes. It was shown that deliquoring of all cakes under study was improved by vibration input. The degree of improvement depends on the material type. The addition of coarse

particles to fine precipitated magnesium oxide significantly enhanced the cake deliquoring by vibration input. Guo et al. [41] also reported improved deliqouring of gasification fine slag filter cakes by applying vertical vibrations. An industrial implementation of this method exists in the mining industry in the form of vibration rollers on a belt filter for enhancement of the dewatering of gold tailings [42]. The oscillatory shear parallel to the filter cake surface is not a conventional, industrially established method for the compaction and deliquoring of fine filter cakes and was first investigated by Illies et al. [15,43,44]. Vibration compaction significantly improved the deliquoring of kaolin, ground and precipitated calcium carbonate filter cakes formed on a vacuum filter plate at low pressures, and reduced filter cake cracking. For the moderately compressible kaolin, the compaction effect relative to the initial state after cake formation was considerably higher than for the less compressible calcium carbonate filter cakes, while vibration compaction was more advantageous compared to compaction by squeezing for the calcium carbonate cakes. Moreover, Yildiz et al. [45] transferred the method to a horizontal vacuum belt filter using a developed vibration module, which could significantly improve mechanical deliquoring of precipitated calcium carbonate filter cakes.

Overall, it is clear that the success of a mechanical deliquoring technique depends on the nature of the slurry, e.g., in terms of particle size distribution, particle shape, and material type, which are therefore important factors for the choice of method [3,28]. Given Illies et al.'s [15,43,44] observation of a basic material dependency of the effectiveness of vibration compaction as for the other mechanical deliquoring methods, it is now necessary to systematically investigate the influence of material properties on the compaction behavior under oscillatory shear. This work deals with the influence of particle size distribution on the compaction effect under vibration input parallel to the cake surface to deepen the process knowledge and to further clarify its applicability. For this purpose, experimental studies were carried out with the laboratory apparatus developed by Illies et al. [43] with five calcium carbonate materials differing in their mean particle size and width of particle size distribution. Material compressibility by squeezing was also investigated to compare the compaction effect under oscillatory shear and squeezing as a function of the particle size distribution. Furthermore, the impact of increasing the agglomeration state for an improved slurry filterability on the compaction behavior under oscillatory shear was investigated.

2. Materials and Methods

2.1. Particle Systems and Slurry Preparation

The particle systems used were ground calcium carbonates with a solid density of 2700 kg/m^3. All model materials exhibited an angular, irregular particle shape, which can be seen as an example for material 4 in Figure 1. Vibration input is effective for cake compaction of this material type according to Illies [44], and a wide range of these materials is available. Therefore, ground calcium carbonates are suitable as model materials to investigate the influence of the particle size distribution on the compaction behavior under oscillatory shear. The median diameter ($x_{50,3}$) and $span = \frac{x_{90,3}-x_{10,3}}{x_{50,3}}$ are used to characterize the particle size distribution. Figure 1 shows the particle size distribution of particle systems dispersed in deionized water measured by a HELOS H0309 laser diffraction instrument (Sympatec GmbH, Clausthal-Zellerfeld, Germany). Table 1 summarizes the characteristic particle size distribution parameters of the particle systems. To determine correlations between mean particle size and compaction behavior, we used materials 1, 2, and 3, which have different median diameters, ranging from 2.3 to 23.5 µm, with approximately the same distribution width of 2.6 to 3.7. The median diameters of materials 4 and 5 are nearly identical, while the distribution width differs significantly, with 4.2 for material 4 and 9.5 for material 5. Thus, these particle systems were suitable for experimental investigations regarding the influence of the distribution width on the compaction success by oscillatory shear. The choice of materials was oriented according to Tiller and Yeh [16], who specified compressible behavior for materials in an average particle size range below 10–20 µm.

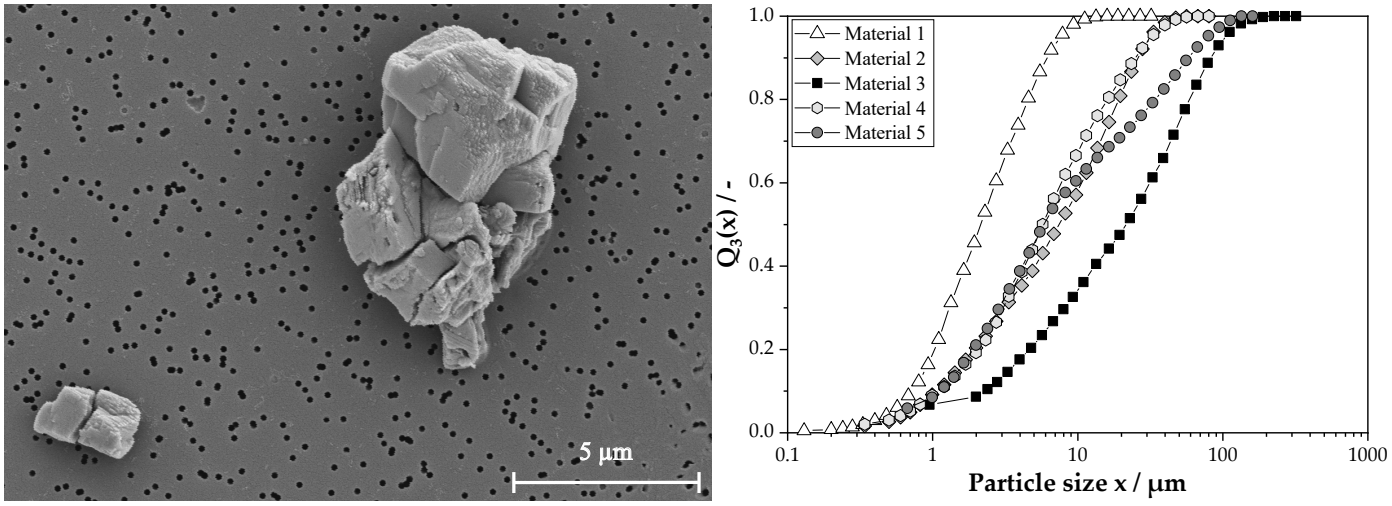

Figure 1. Particles of material 4 captured by scanning electron microscope (**left**). Particle size distribution of the investigated model materials measured by a HELOS H0309 laser diffraction instrument (Sympatec GmbH, Clausthal-Zellerfeld, Germany) (**right**).

Table 1. Median diameter ($x_{50,3}$) and width of particle size distribution (*span*) of the model materials.

Model Material	$x_{50,3}$/µm	span/-
Material 1	2.3	2.6
Material 2	8.2	3.3
Material 3	23.5	3.7
Material 4	6.3	4.2
Material 5	6.5	9.6

For the preparation of the slurries, the model products were suspended in deionized water using an RCT basic magnetic stirrer (IKA Werke GmbH & Co. KG, Staufen, Germany). The solid volume fraction of the suspensions was based on Wiedemann [12] and Illies [44]. To avoid segregation effects during cake formation, the solid volume fraction was 20% for the slurries of materials 1 and 2 and 40% for materials 3, 4, and 5, with higher amounts of coarse particles. Table 2 lists the properties of the prepared slurries. The zeta potential was measured at 20 °C using a Pen Kem 501 instrument (Collotec Meßtechnik GmbH, Niddatal, Germany). A Seven2Go S2 pH measurement instrument (Mettler Toledo, Columbus, OH, USA) and an LF microprocessor conductivity meter (Xylem Inc., Rye Brook, NY, USA) provided the measured values for the pH and electrical conductivity of the slurries at 20 °C, respectively.

Table 2. Properties of the prepared slurries.

Model Material	Zeta Potential /mV	pH /-	Conductivity /µS/cm	Volume Fraction /%
Material 1	−19.0 ± 0.4	8.9 ± 0.2	31.8 ± 6.7	20
Material 2	−20.1 ± 0.7	9.0 ± 0.2	26.3 ± 3.7	20
Material 3	−18.1 ± 0.3	9.0 ± 0.2	30.9 ± 2.1	40
Material 4	−23.9 ± 0.3	8.0 ± 0.5	40.0 ± 0.9	40
Material 5	−21.1 ± 0.1	8.5 ± 0.0	36.8 ± 0.1	40

Particle agglomeration is used to improve the filterability of fine particle slurries in cake filtration [46]. Larger agglomerates increase the cake porosity and reduce the flow resistance during cake formation. Particle agglomeration is achieved, for example, by increasing the electrical conductivity when salts are added. In order to examine how an increase in particle agglomeration affects the compaction behavior under oscillatory

shear, another slurry of material 1 was prepared by adding a sodium chloride solution to the original slurry. This resulted in a slurry with a sodium chloride concentration of 0.014 mol/L, an electrical conductivity of 1292 µS/cm, and a pH of 9.1 at 20 °C. The choice of sodium chloride concentration was based on preliminary experiments wherein the porosity was investigated after cake formation of slurries with different sodium chloride concentrations in the laboratory apparatus (see Section 2.3). The cake porosity no longer rises at a sodium chloride concentration above 0.014 mol/L.

2.2. Press Compaction in the Compression-Permeability Cell

For the characterization of the filter cake compressibility under squeezing, experiments were performed in a compression-permeability cell (CP cell). A detailed description of the CP cell, as shown in Figure 2, is provided by Alles [18].

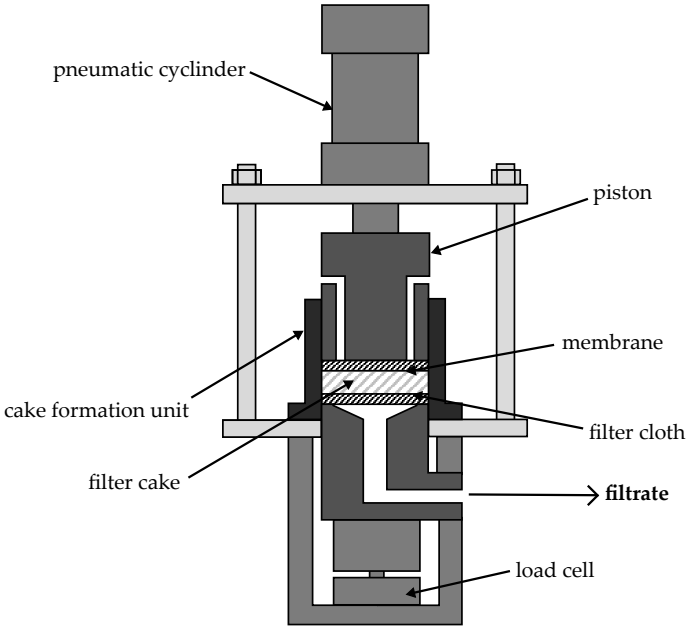

Figure 2. Compression-permeability cell developed and described by Alles [18]. The figure is from Yildiz et al. [45], reprinted with permission of the publisher (Taylor & Francis Ltd., http://www.tandfonline.com).

The slurry was first filled into the cake formation unit with a filter area of 51.5 cm^2. There was a filtrate drain bottom covered with SEFAR NITEX© 03-5/1 monofilament nylon filter cloth (SEFAR AG, Thal, Switzerland).The filter cloth had a mesh size of approximately 5 µm. The filter cake was then compressed by a piston covered with a Supor© 100 hydrophilic polyethersulfone membrane with a pore size of 0.1 µm (Pall Corporation, Port Washington, DC, USA). The initial normal pressure was gradually increased from about 80 kPa up to about 1000 kPa. The compaction in each stage continued until the compaction equilibrium was reached. The duration of each step was set to 60 min for all model materials. The filter cake height (h_c) during compaction was determined by a TLH 100 electrical position sensor (Novotechnik Messwertaufnehmer OHG, Ostfildern, Germany), which continuously measures the piston position.

Equation (1) was used to determine the porosity (ϵ), indicating the compaction degree. Porosity is defined as the pore volume (V_{void}), which is the difference between the total volume (V_{tot}) and the solid volume (V_s), related to the total filter cake volume (V_{tot}). The ratio of the solid mass of the cake (m_s), which is determined by cake drying at 100 °C in the oven for 24 h and cake weighing after the experiment, and the solid density (ρ_s) corresponds to the solid volume. The total cake volume (V_{tot}) can be determined by the product of the filter area (A) and the cake height (h_c).

$$\epsilon = \frac{V_{void}}{V_{tot}} = \frac{V_{tot} - V_s}{V_{tot}} = 1 - \frac{\frac{m_s}{\rho_s}}{Ah_c} \quad (1)$$

To describe the compression behavior under squeezing of filter cakes, modeling the porosity change over the pressure by using Equation (2) is a suitable method according to Tiller et al. [47].

$$(1 - \epsilon) = (1 - \epsilon_0) \cdot (1 + \frac{p}{p_0})^{\beta} \quad (2)$$

While β and p_o are fitting parameters, ϵ_0 represents the porosity in the unloaded state. Tiller et al. [47] denoted the fitting parameter (β) as a compressibility coefficient, which indicates the degree of filter cake compressibility and is thus useful for classifying the compressibility of different materials. A widely used sedimentation experiment in a cylinder was performed, as described by Reichmann and Tomas [48], Alles [18], and Illies [44], to determine the porosity of the sediment in the consolidation equilibrium as an approximation for ϵ_0.

2.3. Compaction by Oscillatory Shear at Low Pressure

Vibration compaction of the filter cakes was studied in the laboratory apparatus (see Figure 3) developed and described in detail by Illies et al. [43]. First, a filter cake with a height of approx. 7.5 mm was formed at a pressure difference of 80 kPa provided by a vacuum in the filter plate. On the filter plate, there was a stainless steel mesh with a width of 1 mm (GKD—Gebr. Kufferath AG, Düren, Germany), which was covered with SEFAR NITEX© 03-5/1 filter cloth as in the CP cell. After cake formation, the transfer plate was placed on the filter cake to apply oscillatory shear at low pressure to the filter cake. Vibration compaction was performed at a constant shear length (l_s) of 4.5 mm, as determined by the eccentricity of the eccentric (e) and the lever dimensions (s_1) and (s_2) by Equation (3), for frequencies of 5, 17, and 40 Hz and for different numbers of oscillations.

$$l_s = 2e \cdot \frac{s_2}{s_1} \quad (3)$$

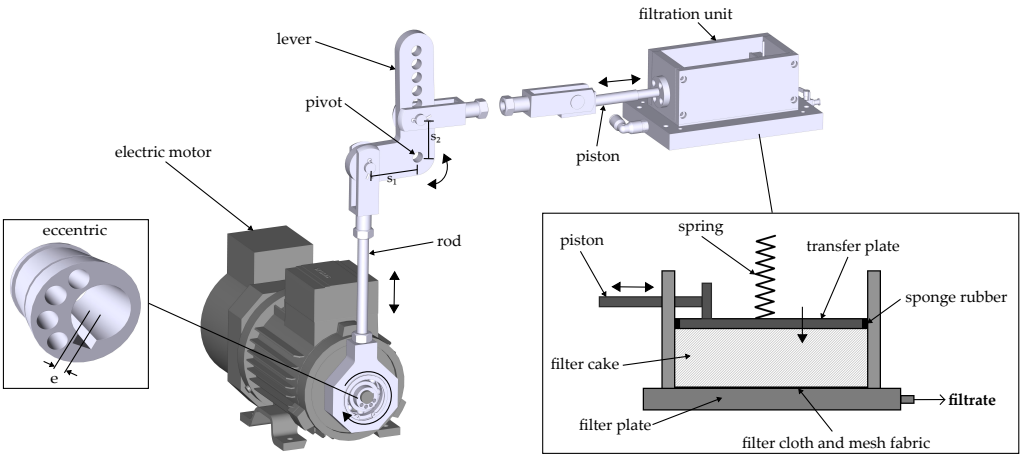

Figure 3. Laboratory apparatus for vibration compaction of compressible filter cakes developed by Illies et al. [43]. The figure is from Yildiz et al. [45], reprinted with permission of the publisher (Taylor & Francis Ltd., http://www.tandfonline.com).

A spring provides a defined contact between the transfer plate and the filter cake. During vibration input, a pressure difference of 80 kPa was applied in the vacuum filter plate to suck off the filtrate. As the sponge rubber and the transfer plate did not completely seal the entire filter cake surface, the suction of the plate by the pressure difference in the vacuum plate was negligible. Thus, the spring and the weight of the plate provided a low compressive pressure of only approx. 3 kPa during vibration compaction. The effect of the normal pressure for compaction was negligible. Superimposed compaction due to

cake shrinkage in the normal range could not be observed for any of the materials at the applied pressure difference. As the pressure difference of 80 kPa exceeded the capillary entry pressure of material 3 in contrast to the other materials, a superimposed desaturation took place during the vibration compaction, so the pressure difference was set to 20 kPa in the vacuum plate in this case. Thus, the influence of desaturation, which leads to increased shear strength on the vibration compaction due to capillary forces according to Oczan et al. [49,50], should be prevented. However, with material 3, it was possible to compare desaturation by a gas pressure difference of 80 kPa with vibration compaction. For this purpose, tests were carried out wherein the cake was desaturated for different times at a pressure difference of 80 kPa after cake formation at 80 kPa.

To evaluate the compaction effect of vibration application, the porosity of the filter cakes was determined as in the CP cell. For this purpose, a filter cake sample was taken with a cylindrical sampler with a diameter of 12 mm. As all filter cakes were in the saturated state during vibration compaction and, thus, the void volume was completely filled with the liquid volume (V_l), the porosity (ϵ) was calculated by Equation (4). The solid volume (V_s) and the total volume (V_{tot}) were calculated using the solid density (ρ_s), the liquid density (ρ_l), the liquid mass (m_l), and the solid mass (m_s). The solid and liquid masses were obtained from gravimetric analysis before and after drying the sample in an oven at 100 °C for 24 h.

$$\epsilon = \frac{V_{void}}{V_{tot}} = \frac{V_{tot} - V_s}{V_{tot}} = 1 - \frac{\frac{m_s}{\rho_s}}{\frac{m_s}{\rho_s} + \frac{m_l}{\rho_l}} \tag{4}$$

For the desaturation experiments with material 3, the displacement of the liquid from the pores occurred without compacting the cake, which is why, in this case, the residual moisture (RM) was compared rather than the porosity. The residual moisture (RM) relating the mass of liquid in the cake (m_l), which is the difference between the total cake mass (m_{tot}) and the solid cake mass (m_s), to the total cake mass (m_{tot}) was calculated according to Equation (5). The solid mass (m_s) and the total cake mass (m_{tot}) were determined by sampling using a cylindrical sampler and subsequent gravimetric analysis before and after drying in an oven at 100 °C for 24 h in the same way as for the porosity analysis.

$$RM = \frac{m_l}{m_{tot}} \cdot 100\% = \frac{m_{tot} - m_s}{m_{tot}} \cdot 100\% \tag{5}$$

3. Results and Discussion

3.1. Characterization of Filter Cake Compressibility under Squeezing

Figure 4 shows the porosity of the different materials under squeezing over the applied compressive pressure. The solid lines represent the approximation of the experimental data using Equation (2) to describe the compressibility of the materials. The parameters of the modeling can be found in Table 3. The porosity values of material 1 with and without the addition of sodium chloride ions at 79 and 73 kPa are not included in the modeling, as they differ significantly from the rest of the data. It can be expected that in the low pressure range, which cannot be fully recorded due to high friction in the apparatus used, there is a slightly different gradient of the porosity. This indicates a compression mechanism in the low pressure range, which differs from the mechanism in the compression pressure range above 100 kPa. Alles [18], Wiedemann [12], and Illies [44] showed that the compression mechanisms can differ depending on the pressure range and can be recognized by a change in the gradient.

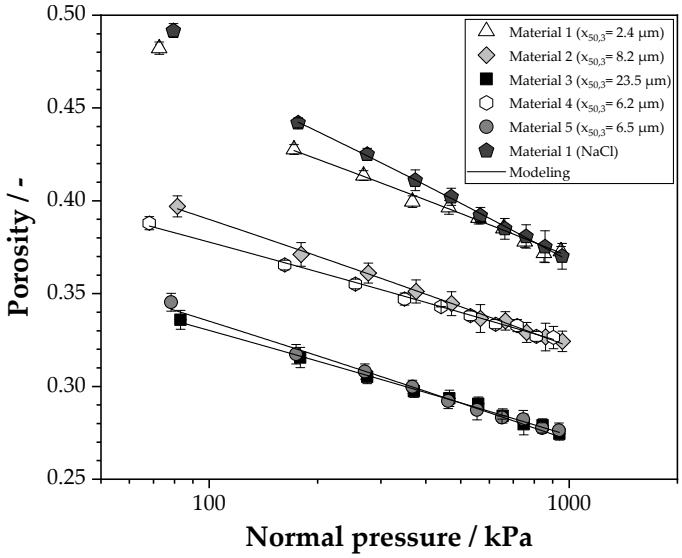

Figure 4. Compressibility of different materials under squeezing. An approximation of the experimental data was obtained with Equation (2).

Table 3. Parameters and corrected coefficients of determination of the data modeling presented in Figure 4 using Equation (2).

Model Material	ϵ_0/-	p_o/-	β/-	R^2/-
Material 1	0.73	0.00026	0.054	0.9909
Material 2	0.60	0.00875	0.046	0.9966
Material 3	0.46	0.18902	0.035	0.9938
Material 4	0.50	0.30706	0.037	0.9955
Material 5	0.56	0.00308	0.040	0.9894
Material 1 (NaCl)	0.75	0.00283	0.073	0.9989

Based on the general porosity level during squeezing and the unloaded state of the materials represented by the reference porosity (ϵ_0) after a sedimentation test, differences in the materials depending on particle size distribution and agglomeration state are noticeable. Considering materials 1, 2, and 3 with different mean particle sizes, it can be seen that more porous structures are formed with decreasing particle size due to higher interparticle forces compared to mass forces, as predicted by Tiller and Yeh [16]. Comparing materials 4 and 5, which differ in their width of particle size distribution, compression achieves significantly lower porosity values for the widely distributed material 5 than for the narrowly distributed material 4. This observation has been previously reported in the literature [51,52] and can be explained by the fact that smaller particles fill the voids between larger particles, resulting in a more compacted state. The targeted increase in porosity by the addition of sodium chloride to the material 1 slurry can also be clearly detected.

The compressibility of the materials, characterized by the compressibility index (β), can be classified as low to moderate according to Tiller et al. [47]. For materials 1, 2, and 3, it is found that the compressibility increases with decreasing mean particle size. This observation is consistent with the findings of Tiller and Yeh [16], who stated that more porous structures can be compressed to a higher degree. The widely distributed material 5 has a slightly higher compressibility in contrast to the narrowly distributed material 4, which is also a result of the filling of the void volume between coarse particles by fine particles. Material 1 is more compressible with added sodium chloride ions, resulting mainly from the more porous structure in the unloaded state. Compression with higher normal pressures achieves approximately the same compression states as for material 1 without added sodium chloride ions.

3.2. Influence of the Mean Particle Size on the Compaction Behavior under Oscillatory Shear

The cake porosity of materials 1, 2, and 3 with different mean particle sizes ($x_{50,3}$) after cake formation at 80 kPa (0 oscillations) and vibration compaction at a shear length of 4.5 mm for different numbers of oscillations and frequencies can be found in Figure 5. For the values of material 1 after vibration compaction at 40 Hz, it should be noted that before the vibration application at 40 Hz, the first 1000 oscillations were applied to the filter cake at 17 Hz. Due to the high residual cake moisture of material 1 after cake formation, direct vibration input at the high frequency of 40 Hz caused a fluidization of the filter cake at the beginning. As a result, parts of the filter cake were discharged at the sides of the transfer plate and were not compacted.

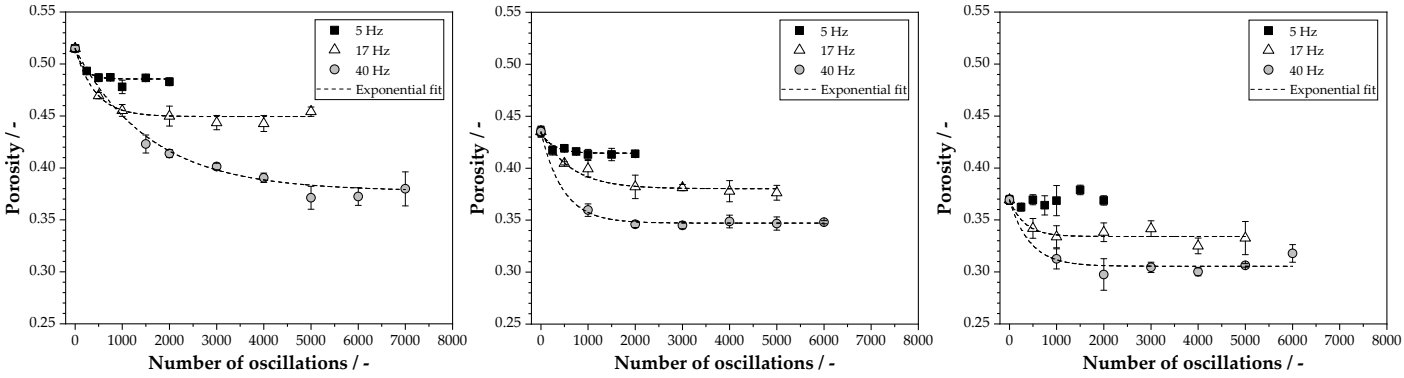

Figure 5. Filter cake porosity of material 1 ($x_{50,3}$ = 2.3 µm, **left**), material 2 ($x_{50,3}$ = 8.2 µm, **center**), and material 3 ($x_{50,3}$ = 23.5 µm, **right**) after cake formation and vibration compaction at a constant shear length of 4.5 mm. The dashed line illustrates the exponential fit obtained using Equation (6).

The reference porosities after cake formation demonstrate the identical differences between the materials observed in Section 3.1. As expected, material 1 with the smallest mean particle size forms highly porous filter cakes. The cake porosities of materials 2 and 3 after cake formation decrease accordingly with increasing mean particle size. For all materials, a significant porosity decrease and, thus, a compaction effect of vibration application can be identified with an increasing number of oscillations until a steady-state compaction equilibrium is reached for each frequency. As the frequency increases, the compaction effect of vibration rises. Only for material 3 with the highest mean particle size is there no apparent effect of vibration compaction at 5 Hz.

Exponential kinetics are typical for vibration compaction and were previously observed by Illies et al. [43] and Yildiz et al. [45]. According to Illies et al. [43], Equation (6) is useful to describe the exponential decrease in porosity as a function of the number of vibrations (n):

$$\epsilon(n) = \epsilon_\infty + B \cdot e^{-\frac{n}{\vartheta}} \tag{6}$$

where (ϵ_∞) is the minimum achievable porosity in the compaction equilibrium for the investigated frequency; (B) expresses the consolidation potential, which is the difference between the reference porosity after cake formation (ϵ_0) and the minimum achievable porosity (ϵ_∞); and (ϑ) is another fitting parameter. The parameters and the corrected coefficients of determination of the fit are listed in Tables A1–A3 in Appendix A. It can be observed that lower minimum porosity values are achievable at the same frequency with increasing mean particle size. The finer the particles, the larger the interparticle forces compared to the mass forces of the particles. The application of oscillatory shear must overcome the interparticle forces to induce particle rearrangement and, thus, to put the cake in a more compacted state. However, if the frequency and, thus, the energy input are sufficiently high, vibration compaction achieves comparable compaction states for a finer material as for a coarser material at a lower frequency, as illustrated by the examples of material 1 at 40 Hz and material 2 at 17 Hz.

Since the reference porosities of the materials after cake formation, which represent the initial states before vibration compaction, are different, the consolidation potential related to the reference porosity must be regarded to evaluate the compaction effect. The related consolidation potential (b) is calculated from the difference between the reference porosity (ϵ_0) and the minimum porosity (ϵ_∞) reached by vibration compaction divided by the reference porosity (ϵ_0) (see Equation (7)). For the difference between the reference porosity (ϵ_0) and the minimum achievable porosity (ϵ_∞), the consolidation potential (B) determined by the exponential fit is used.

$$b = \frac{\epsilon_0 - \epsilon_\infty}{\epsilon_0} \cdot 100\% = \frac{B}{\epsilon_0} \cdot 100\% \tag{7}$$

The related consolidation potential of the materials as a function of the frequency is given in Figure 6. In the case of the vibration compaction of material 3 at 5 Hz, a consolidation potential of 0 is assumed, since no compaction effect of vibration is evident at this frequency (see Figure 5 on the right).

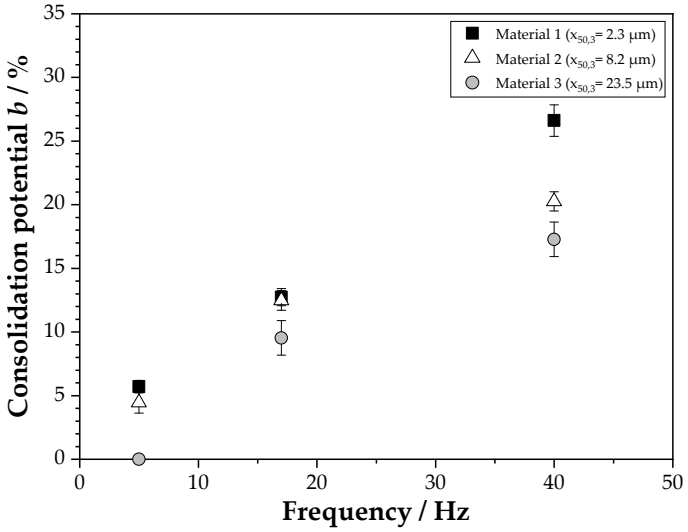

Figure 6. Consolidation potential (b) of materials 1, 2, and 3 under oscillatory shear for different frequencies.

For all frequencies, vibration compaction achieves a significantly higher consolidation potential for the two finer (materials 1 and 2) than for the coarse material 3. There is hardly any difference between the consolidation potential at 5 and 17 Hz between the finer materials 1 and 2. Vibration input at 40 Hz reduces the initial cake porosity of the finest material 1 by 26.6 ± 1.2 %, while for the coarser material 2, a much lower consolidation potential of about 20.3 ± 0.8 % is achieved. It can thus be concluded that the compactibility under oscillatory shear increases with decreasing mean particle size. The initial highly porous structures of finer materials provide the particles with a high pore volume in which they can move induced by the vibration input and thus adopt a higher state of compaction. Hence, compaction under oscillatory shear acts as a function of the mean particle size identically to compaction under compression according to Tiller and Yeh [16] and as shown in Section 3.1.

Compaction, as a mechanical deliquoring method of compressible filter cakes, is usually realized by squeezing the cake. As a result, alternative vibration compaction competes with conventional cake compression. Therefore, the achievable compaction states of the materials by squeezing and vibration should be compared to check how the mean particle size affects the benefit of vibration compaction compared to compaction by squeezing. The achievable compaction states at different normal pressures in the CP cell shown in Figure 4 are used as comparative values for compaction by squeezing. It should be mentioned that compaction by squeezing in industrial reality is quite different from the idealized compaction process in the CP cell. Elastic recovery effects of the cake, which act, for example, in belt filter presses or in

indexing belt filters with hydraulic press modules after the compressive load is removed, are not taken into account in the CP cell, as the compaction states were determined during the load. Furthermore, with regard to frame or chamber filter presses, it should be considered that in the CP cell, the load is applied by a piston and not by the hydraulic pressure of a slurry pump. Thus, compaction in the CP cell is an idealized process, which is nevertheless suitable for rough estimation of compaction of the materials by squeezing compared to vibration compaction.

Figure 7 compares the cake porosities of the three materials obtained by squeezing in the CP cell for different normal pressures and by vibration compaction for different frequencies at a constant normal pressure of approx. 3 kPa. As vibration application to material 3 does not lead to any compaction, no calculation of the minimum porosity is possible using Equation (6). Thus, no values for 5 Hz are shown in the right plot. The equivalent normal pressure is the pressure required to achieve the same compaction state of vibration compaction at a certain frequency by squeezing. For determination of the equivalent normal pressure, Equation (2) with the fitting parameters of the respective material from Table 3 is used. For fine materials 1 and 2, vibration compaction in the low to medium frequency range from 5 to 17 Hz only achieves compaction states that squeezing already reaches at normal pressures below 200 kPa. The equivalent normal pressure of vibration compaction in the same frequency range is even lower, at about 80 kPa, for the coarsest material 3 in contrast to the finer materials. However, the vibration compaction of material 1 at 40 Hz reaches identical compaction states as the squeezing of the filter cake up to the maximum pressure of 1000 kPa. For material 2, the equivalent normal pressure at 40 Hz of about 434 kPa is significantly lower than for material 1, while the equivalent normal pressure at 40 Hz is only 279 kPa for the coarse material 3. The smaller the mean particle size of the material, the more vibration compaction can keep up with compaction by squeezing. High normal pressures for the compaction of compressible filter cakes are not feasible on existing horizontal indexing belt filters due to the high load. Vibration compaction can also be realized in the high frequency range by using a vibration module on existing indexing belt filters, as successfully demonstrated by Yildiz et al. [45]. Thus, the benefit of vibration input to compact cakes at much lower normal pressures compared to squeezing at high normal pressures increases with decreasing mean particle size.

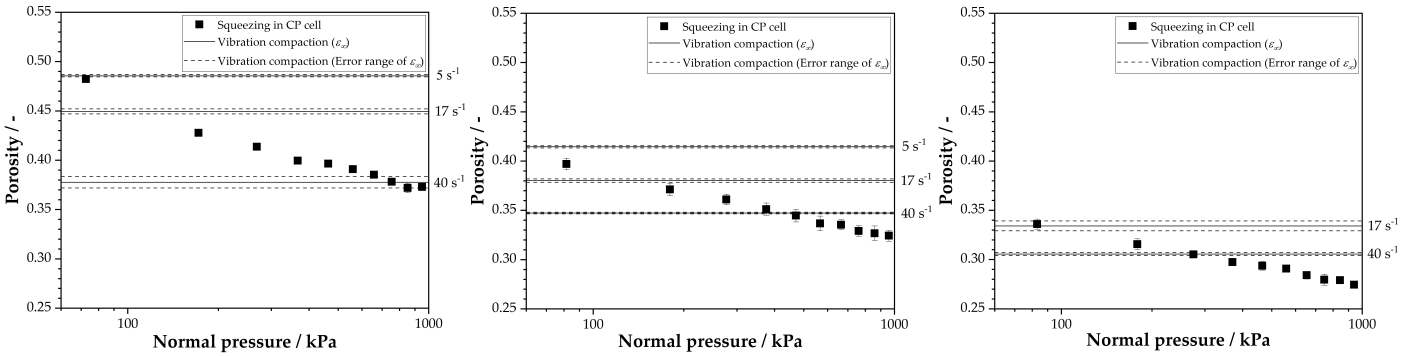

Figure 7. Minimal achievable porosity of material 1 (**left**), material 2 (**center**), and material 3 (**right**) by squeezing in the CP cell for different normal pressures (black data points) and by vibration compaction for different frequencies at a constant normal pressure of approx. 3 kPa. The horizontal solid line illustrates the minimum porosity (ϵ_∞) determined by the exponential fit, and the horizontal dashed line shows the corresponding error range of (ϵ_∞) (see Tables A1–A3).

3.3. Influence of the Width of Particle Size Distribution on Compaction Behavior under Oscillatory Shear

Materials 4 and 5 with the same mean particle size and a different width of particle size distribution were used to analyze the influence of the distribution width on compaction behavior under oscillatory shear. Figure 8 displays the compaction kinetics of the two materials under oscillatory shear.

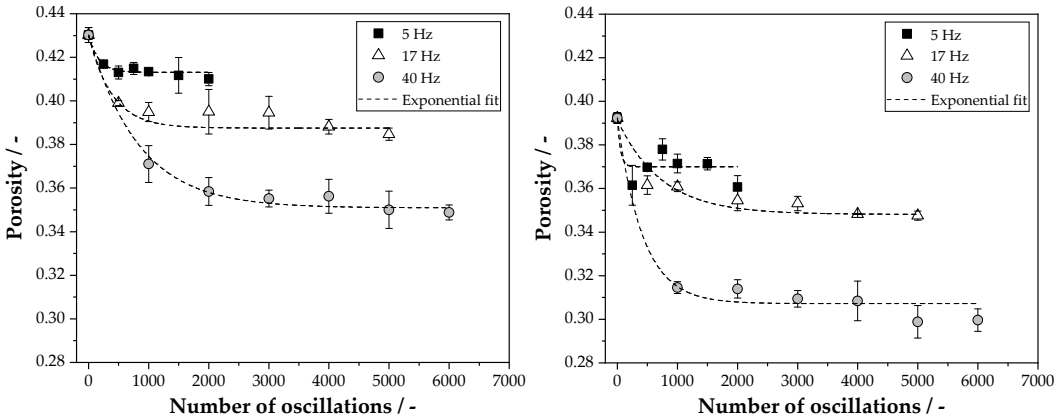

Figure 8. Filter cake porosity of material 4 (*span* = 4.2, **left**) and material 5 (*span* = 9.6, **right**) after cake formation and vibration compaction at a constant shear length of 4.5 mm. The dashed line illustrates the exponential fit obtained using Equation (6).

Differences between the filter cakes of materials 4 and 5 already arise after cake formation. Since material 5 has a wide particle size distribution and smaller particles fill the pore volume between the larger particles, this results—as known from the literature [51,52]—in a more compacted filter cake with lower porosity after cake formation in contrast to the more narrowly distributed material 4. Vibration input produces cake compaction for both materials that increases with an increasing number of oscillations and increasing frequency. The characteristic exponential compaction kinetics, as a function of the number of oscillations, which can be modeled using Equation (6), can also be seen here. Tables A4 and A5 in Appendix A list the parameters and corrected coefficients of determination of the fit. Similar to the compaction by squeezing (see Section 3.1), the compaction states of the widely distributed material 5 caused by the vibration input are significantly lower than those of the narrowly distributed material 4. The reason is also that for the widely distributed materials, more void volume is available between larger particles, where smaller particles can move, stimulated by the vibration input.

As reported in Section 3.2, different reference porosities after cake formation require an assessment of the compaction effect based on the related consolidation potential (b) plotted against the frequency in Figure 9. Vibration compaction at 5 and 17 Hz has a slightly higher compaction effect for the widely distributed material 5 than for the narrowly distributed material 4. However, there is a clearly higher compaction effect for the widely distributed material 5 at 40 Hz. This fact is surprising, considering the higher initial pore volume of the narrowly distributed material 4 after cake formation, which favors the compressibility under oscillatory shear, as noticed in Section 3.2. Due to the greater width of particle size distribution of material 5, the effect of filling the void volume between larger particles with small particles predominates, resulting in a higher related consolidation potential despite the lower initial porosity. Thus, in addition to the initial void volume after cake formation caused by particle fineness, the width of particle size distribution is also decisive for the consolidation potential under oscillatory shear.

Pearce [40] analyzed vibration application perpendicular to the filter cake surface to improve mechanical deliquoring by filter cake compaction in a laboratory filter press and in a vacuum filter. It was found that vibration application leads to higher compaction or deliquoring effects of magnesium hydroxide cakes by adding coarser particles. The investigations of the vibration input perpendicular to the cake surface concerning the influence of the width of particle size distribution on the compaction success are thus in line with the observations shown here for the vibration input parallel to the cake surface.

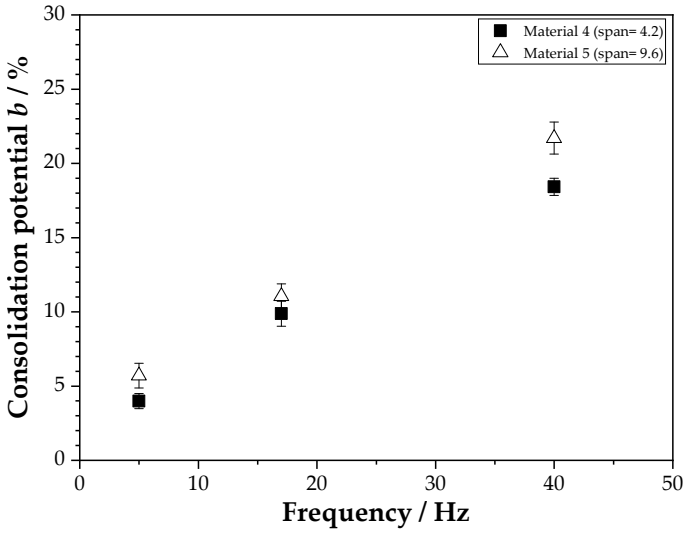

Figure 9. Consolidation potential (b) of materials 4 and 5 under oscillatory shear for different frequencies.

A comparison of the achievable porosities by squeezing in the CP cell and by vibration compaction is provided in Figure 10. For both materials, the vibration input at 5 and 17 Hz only provides compaction, which is already achieved by squeezing in the CP cell at normal pressures below 80 kPa. At the highest frequency of 40 Hz, the equivalent normal pressure of vibration compaction is minimally higher, at about 315 kPa for the narrowly distributed material 4 in contrast to 281 kPa for the widely distributed material. Tendentially, the vibration compaction of a narrowly distributed material can keep up with compaction by squeezing a bit more than for a widely distributed material. Material 2 has a similar mean particle size as both materials 4 and 5, although material 2 is more narrowly distributed. Despite the slightly larger mean particle size, the equivalent compaction pressure of material 4 at 40 Hz is 434 kPa, which is significantly higher than for materials 4 and 5. It becomes clear here that vibration compaction of narrowly distributed materials can compete with compaction by squeezing to a greater extent.

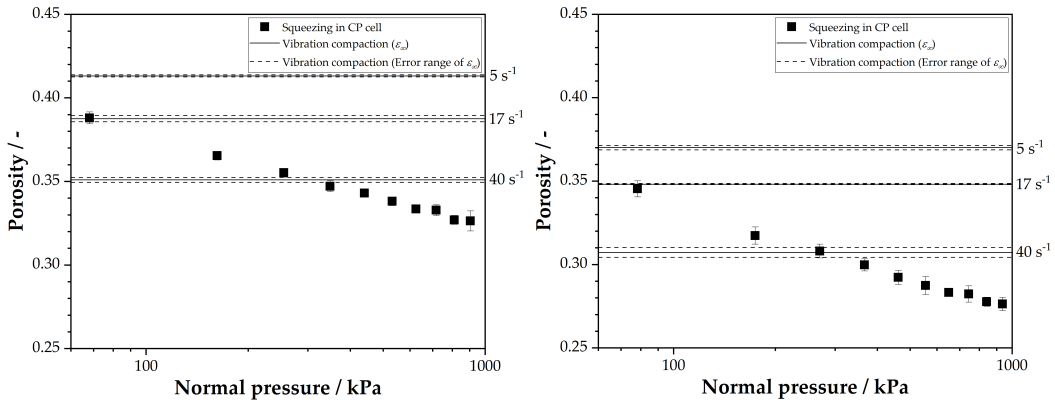

Figure 10. Minimal achievable porosity of material 4 (**left**) and material 5 (**right**) by squeezing in the CP cell for different normal pressures (black data points) and by vibration compaction for different frequencies at a constant normal pressure of approx. 3 kPa. The horizontal solid line illustrates the minimum porosity (ϵ_∞) determined by the exponential fit, and the horizontal dashed line shows the corresponding error range of (ϵ_∞)

3.4. Impact of Increasing the Agglomeration State on the Compaction Effect of Oscillatory Shear

The compaction kinetics of material 1 without and with the addition of sodium chloride ions under oscillatory shear to increase the particle agglomeration state can be found in Figure 11.

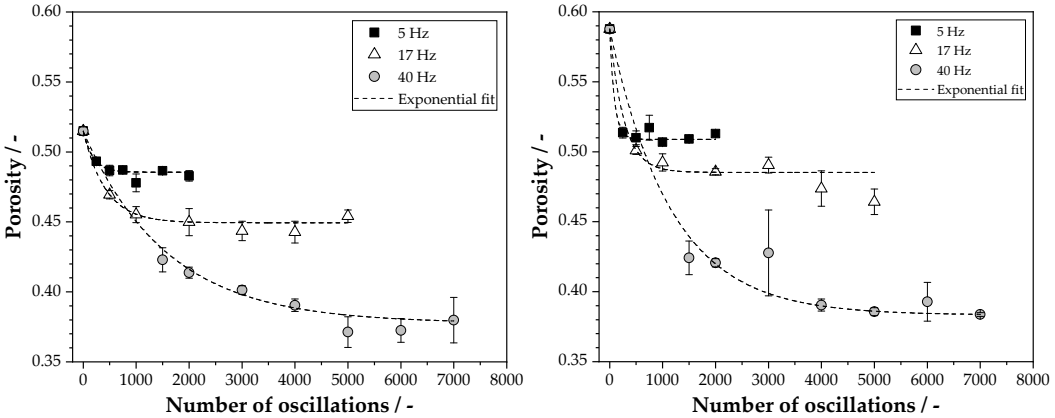

Figure 11. Filter cake porosity of material 1 without (**left**) and with added sodium chloride ions (**right**) after cake formation and vibration compaction at a constant shear length of 4.5 mm. The dashed line illustrates the exponential fit obtained using Equation (6).

As expected, material 1 with higher particle agglomeration achieved by adding sodium chloride ions forms a significantly more porous cake after cake formation. Despite the increased particle agglomeration, a significant compaction effect is observed for material 1 with the added sodium chloride ions due to the vibration input, which typically increases with rising frequency. Vibration input at 5 and 17 Hz provides higher minimum porosities in the case of the highly agglomerated material 1 (see Tables A1 and A6 in Appendix A) compared to material 1 without added sodium chloride ions. After vibration compaction at 40 Hz, where the first 1000 vibrations were also applied to the cake at 17 Hz, the achievable minimum porosity is almost identical to that of material 1 without sodium chloride ions. This means that in the low frequency range, the compaction effect of the material is limited due to increased particle agglomeration. If the frequency and thus the energy input are sufficiently high, the adhesive forces are overcome to a greater extent, and the compaction-determined mechanism of particle rearrangement is supported, whereby the same compaction of the material can be achieved as without added sodium chloride ions. The related consolidation potential of the strongly agglomerated material is, of course, significantly larger due to the higher porosity after cake formation. This confirms, as previously observed in Section 3.2, that a high initial porosity after cake formation has a basically positive effect on the consolidation potential under oscillatory shear. A comparison of the minimum achievable porosities by vibration compaction and by squeezing in the CP cell is omitted, since both compaction methods allow identical compaction states in both cases at sufficiently high normal pressures or frequencies.

3.5. Comparison of the Compaction or Deliquoring Results by Oscillatory Shear to Other Mechanical Methods

Besides compaction by oscillatory shear, there are other mechanical methods for cake compaction and deliquoring, such as deliquoring by a gas pressure difference, squeezing, steady shear at a normal pressure, or vibration application perpendicular to the filter surface, which were mentioned in the Introduction in Section 1. However, a comparison of compaction and deliquoring results of the materials under oscillatory shear with other methods is only possible in isolated cases because ground calcium carbonate products such as those used in this study with a similar particle size range and the same particle shape were used only in a few cases.

Vibration compaction is particularly designed to improve the deliquoring of compressible filter cakes on widely used vacuum-based cake filtration apparatuses such as belt filters [45]. In this case, deliquoring by a gas pressure difference after cake formation is limited to a pressure difference of 80 kPa. Since the capillary entry pressure is only exceeded for filter cakes of the coarsest material 3 at this pressure difference causing cake desaturation, a comparison was only carried out for this material.

Figure 12 shows the cake residual moisture of material 3 achieved by the application of oscillatory shear or deliquoring by desaturation at a gas pressure difference at 80 kPa after cake formation (0 s). Similar to vibration compaction, the residual moisture is exponentially reduced by desaturation until a state of equilibrium is reached after approx. 60 s. The residual moisture after desaturation is in the same range in the equilibrium state as after the application of oscillatory shear at 40 Hz. Thus, vibration compaction can keep up with desaturation for this coarse material. For the other materials studied, where desaturation by applying gas pressure difference is not possible and, thus, the residual moisture remains constant after cake formation, vibration compaction has a clear advantage, as shown by the significant reduction in porosity, further displacing liquid from the cake.

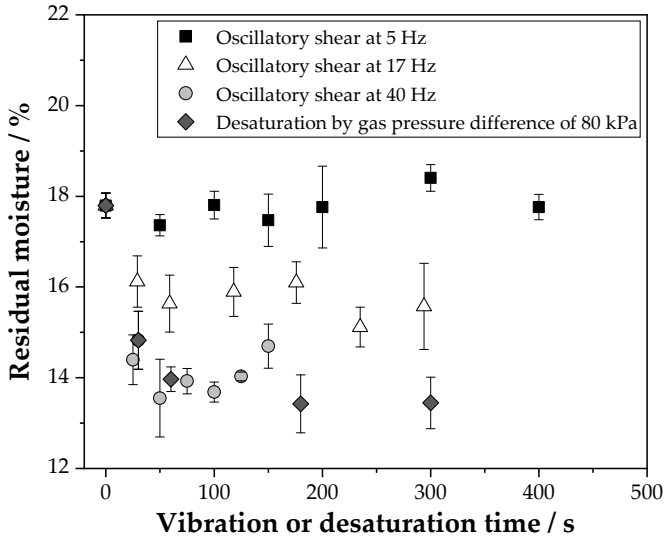

Figure 12. Residual moisture of material 3 achieved by oscillatory shear and by the application of a gas pressure difference of 80 kPa.

The use of steady shear with simultaneous squeezing to compact ground calcium carbonate products was investigated by Hammerich et al. [31,32] in a lab-scale press shear cell. Steady shear at a shear rate of 1.5 mm/min at a normal pressure up to 60 kPa results in an average porosity of 0.4 for a ground calcium carbonate product with a mean particle size ($x_{50,3}$) of about 6 µm. The oscillatory shear at 17 and 40 Hz achieves significantly lower porosities of approx. 0.39 and 0.35 for the exact same material 4 at a lower superimposed normal pressure of 3 kPa compared to steady shear. Compaction by continuous shear at significantly higher normal pressures was not considered for this product. However, it should be noted that the implementation of the method at higher normal pressures on industrial cake filtration apparatuses such as drum or belt filters is difficult. The apparatus must be designed to handle these high loads, requiring additional costs. However, vibration compaction can be implemented on existing filtration apparatuses, such as a belt filter, as demonstrated by Yildiz et al. [45].

The High Pressure Dewatering Rolls developed and tested by Höfgen et al. [34] compact a ground calcium carbonate product corresponding to material 3 used in the present study via a combination of squeezing at a hydraulic pressure of 3000 kPa and steady shear to a solid volume concentration of about 0.63. In this case, the application of oscillatory shear at 17 and 40 Hz also achieves significantly higher compaction at much lower normal pressure to solid volume concentrations of 0.67 and 0.69. Since continuous operation, such as in High Pressure Dewatering Rolls, is also possible for vibration compaction, as shown by Yildiz et al. [45], the use of oscillatory shear is more advantageous for this material.

4. Conclusions

The results of this study show correlations between the compaction success of compressible materials under oscillatory shear and their particle size distributions. The consolidation

potential of vibration compaction related to the initial state after cake formation increases with decreasing mean particle size of the material. This is predominantly related to the high porosity after cake formation of finer materials. The more pore volume available for the particles, the higher the potential to attain a more compact state by particle rearrangement. Besides the mean particle size, the width of particle size distribution also has a decisive influence on the compaction effect by vibration input. Since smaller particles fill the void volume between the larger particles, vibration compaction achieves lower compaction states and a higher related consolidation potential for more widely distributed materials. The influences of the particle size distribution on the compaction behavior both under squeezing and under vibration input are therefore identical. A comparison between the achievable compaction states by squeezing and vibration input reveals that the benefit of oscillatory shear compared to compression grows with decreasing mean particle size and width of particle size distribution. Comparisons of oscillatory shear with other mechanical methods demonstrated that in the case of ground calcium carbonates, vibration compaction achieves comparable or even significantly better compaction or deliquoring results. Increased particle agglomeration is particularly used for fine materials prior to cake filtration to improve the slurry filterability in industry. However, if the energy input is sufficiently high, identical compaction conditions as without slurry pretreatment are possible despite the increased particle agglomeration, which underlines the industrial suitability of the process.

It should be noted that apart from the particle size distribution, the particle shape is also crucial for cake compaction, which can cause the compaction behavior under squeezing and under oscillatory shear to differ, as Illies et al. [15,43,44] demonstrated for three different material types. However, other material classes should be investigated in terms of compactibility by vibration application to further investigate the applicability of the technique. Furthermore, the influence of pre-desaturation on the compaction behavior under oscillatory shear should be studied in the future, which can lead to an increase in the shear strength of the filter cake according to Oczan et al. [49,50]. The effect of vibration compaction has been studied only for fully saturated cakes. In the case of products such as material 3, whose capillary entry pressure can be exceeded in the pressure difference range of vacuum cake filtration, unintentional pre-desaturation cannot be ruled out in the continuous process of drum or belt filters.

Author Contributions: Conceptualization, T.Y.; Methodology, T.Y.; Validation, T.Y. and J.G.; Formal analysis, T.Y.; Investigation, J.G.; Resources, T.Y.; Data curation, T.Y.; Writing—original draft preparation, T.Y.; Writing—review and editing, T.Y., M.G. and H.N.; Visualization, T.Y.; Supervision, H.N.; Project administration, H.N.; Funding acquisition, H.N. All authors have read and agreed to the published version of the manuscript.

Funding: This research was funded by the German Federation of Industrial Research Associations (AiF Arbeitsgemeinschaft Industrieller Forschungsvereinigungen Otto von Guericke e.V.) within the IGF project 20674N "Continuous Vibration Compaction". We acknowledge support from the KIT-Publication Fund of the Karlsruhe Institute of Technology for the funding of the APC.

Data Availability Statement: Not applicable.

Acknowledgments: We thank the publisher Taylor & Francis Ltd. (http://www.tandfonline.com) and the authors for permission to reuse Figures 2 and 3 from "Vibration compaction of compressible filter cakes for mechanical deliquoring on a horizontal vacuum belt filter" by Yildiz et al. [45] published in Drying Technology on 3 February 2023.

Conflicts of Interest: The authors declare no conflict of interest.

Abbreviations

The following abbreviations are used in this manuscript:

CP cell	Compression-permeability cell

Appendix A

Table A1. Parameters of the exponential data fit of material 1 in Figure 5 (left) obtained with Equation (6). The standard errors of the fit indicate the deviations of the minimum porosity (ϵ_∞) and the consolidation potential (B).

Frequency / Hz	ϵ_∞/-	B/-	ϑ/-	R^2/-
5	0.486 ± 0.001	0.029 ± 0.003	186	0.9560
17	0.449 ± 0.003	0.066 ± 0.003	422	0.9850
40	0.378 ± 0.006	0.137 ± 0.006	1578	0.9940

Table A2. Parameters of the exponential data fit of material 2 in Figure 5 (center) obtained with Equation (6). The standard errors of the fit indicate the deviations of the minimum porosity (ϵ_∞) and the consolidation potential (B).

Frequency / Hz	ϵ_∞/-	B/-	ϑ/-	R^2/-
5	0.414 ± 0.001	0.019 ± 0.004	270	0.8246
17	0.380 ± 0.002	0.054 ± 0.003	637	0.9808
40	0.347 ± 0.001	0.088 ± 0.003	465	0.9919

Table A3. Parameters of the exponential data fit of material 3 in Figure 5 (right) obtained with Equation (6). The standard errors of the fit indicate the deviations of the minimum porosity (ϵ_∞) and the consolidation potential (B).

Frequency / Hz	ϵ_∞/-	B/-	ϑ/-	R^2/-
5	-	-	-	-
17	0.334 ± 0.004	0.035 ± 0.005	322	0.8942
40	0.305 ± 0.002	0.064 ± 0.005	429	0.9651

Table A4. Parameters of the exponential data fit of material 4 in Figure 8 (left) obtained with Equation (6). The standard errors of the fit indicate the deviations of the minimum porosity (ϵ_∞) and the consolidation potential (B).

Frequency / Hz	ϵ_∞/-	B/-	ϑ/-	R^2/-
5	0.413 ± 0.001	0.017 ± 0.002	165	0.9255
17	0.388 ± 0.002	0.043 ± 0.004	386	0.9582
40	0.351 ± 0.002	0.079 ± 0.002	833	0.9949

Table A5. Parameters of the exponential data fit of material 5 in Figure 8 (right) obtained with Equation (6). The standard errors of the fit indicate the deviations of the minimum porosity (ϵ_∞) and the consolidation potential (B).

Frequency / Hz	ϵ_∞/-	B/-	ϑ/-	R^2/-
5	0.370 ± 0.001	0.022 ± 0.003	50	0.8860
17	0.348 ± 0.000	0.043 ± 0.003	730	0.9698
40	0.307 ± 0.003	0.085 ± 0.004	418	0.9880

Table A6. Parameters of the exponential data fit of material 1 (NaCl) in Figure 11 (right) obtained with Equation (6). The standard errors of the fit indicate the deviations of the minimum porosity (ϵ_∞) and the consolidation potential (B).

Frequency / Hz	ϵ_∞/-	B/-	ϑ/-	R^2/-
5	0.509 ± 0.001	0.079 ± 0.004	90	0.9881
17	0.485 ± 0.003	0.102 ± 0.004	270	0.9898
40	0.383 ± 0.001	0.204 ± 0.002	1161	0.9992

References

1. Gerl, S.; Stahl, W. Improved dewatering of coal by steam pressure filtration. *Coal Prep.* **1996**, *17*, 137–146. [CrossRef]
2. Couturier, S.; Valat, M.; Vaxelaire, J.; Puiggali, J. Enhanced expression of filter cakes using a local thermal supply. *Sep. Purif. Technol.* **2007**, *57*, 321–328. [CrossRef]
3. Anlauf, H. *Wet Cake Filtration: Fundamentals, Equipment, and Strategies*; John Wiley & Sons: Hoboken, NJ, USA, 2019.
4. Vaxelaire, J.; Bongiovanni, J.M.; Puiggali, J.R. Mechanical dewatering and thermal drying of residual sludge. *Environ. Technol.* **1999**, *20*, 29–36. [CrossRef]
5. Schubert, H. *Untersuchungen zur Ermittlung von Kapillardruck und Zugfestigkeit von feuchten Haufwerken aus körnigen Stoffen*; H. Schubert: Wettringen, Germany, 1972.
6. Lloyd, P.; Dodds, J. Liquid retention in filter cakes. *Filtr. Sep.* **1972**, *9*, 91–96.
7. Rushton, A.; Hameed, M. The effect of concentration in rotary vacuum filtration. *Filtr. Sep.* **1969**, *6*, 136.
8. Anlauf, H.; Bott, R.; Stahl, W.; Krebber, A. Die Bildung von Schrumpfrissen in Filterkuchen bei der Entwässerung feinkörniger Erze. *Aufbereit.-Tech.* **1985**, *26*, 188–196.
9. Barua, A.; Eagles, W.; Giorgio, G.; Stepanek, F. Experimental Study of Filter Cake Cracking during Deliquoring. Ph.D. Thesis, Imperial College London, London, UK, 2013.
10. Wiedemann, T.; Stahl, W. Schrumpfungs-und Rißbildungsverhalten feinkörniger Filterkuchen bei der Gasdifferenzdruckentfeuchtung. *Chem. Ing. Tech.* **1995**, *67*, 1486–1489. [CrossRef]
11. Wiedemann, T.; Stahl, W. Experimental investigation of the shrinkage and cracking behaviour of fine participate filter cakes. *Chem. Eng. Process. Process. Intensif.* **1996**, *35*, 35–42. [CrossRef]
12. Wiedemann, T. Das Schrumpfungs- und Rißbildungsverhalten von Filterkuchen. Ph.D. Thesis, Universität Karlsruhe (TH), Karlsruher, Germany, 1996.
13. Cheremisinoff, N.P. Industrial liquid filtration equipment. In *Fibrous Filter Media*; Elsevier: Amsterdam, The Netherlands, 2017; pp. 27–50.
14. Redeker, D.; Steiner, K.H.; Esser, U. Das mechanische Entfeuchten von Filterkuchen. *Chem. Ing. Tech.* **1983**, *55*, 829–839. [CrossRef]
15. Illies, S.; Anlauf, H.; Nirschl, H. Vibration-enhanced compaction of filter cakes and its influence on filter cake cracking. *Sep. Sci. Technol.* **2017**, *52*, 2795–2803. [CrossRef]
16. Tiller, F.M.; Yeh, C. The role of porosity in filtration. Part XI: Filtration followed by expression. *AIChE J.* **1987**, *33*, 1241–1256. [CrossRef]
17. Wakeman, R.; Thuraisingham, S.; Tarleton, E. Colloid science in solid-liquid separation technology. Is it important? *Filtr. Sep.* **1989**, *26*, 277–283.
18. Alles, C.M. Prozeßstrategien für die Filtration mit Kompressiblen Kuchen. Ph.D. Thesis, Universität Fridericiana Karlsruhe (TH), Karlsruhe, Germany, 2000.
19. Alt, C. Preß-Filterapparate zur Verminderung der Restfeuchte von Filterkuchen. *Chem. Ind.* **1975**, *26*, 422–426.
20. Alt, C. Schlammentwässerung mit Preßfiltern. *Chem. Ing. Tech.* **1976**, *48*, 115–124. [CrossRef]
21. Shirato, M.; Murase, T.; Kato, H.; Fukaya, S. Fundamental analysis for expression under constant pressure. *Filtr. Sep.* **1970**, *7*, 277–282.
22. Shirato, M.; Murase, T.; Negawa, M.; Senda, T. Fundamental studies of expression under variable pressure. *J. Chem. Eng. Jpn.* **1970**, *3*, 105–112. [CrossRef]
23. Riemenschneider, H. Entfeuchten Durch Pressen. Ph.D. Thesis, Universität Stuttgart, Stuttgart, Germany, 1983.
24. Halde, R.E. Filterbelt pressing of sludge: A laboratory simulation. *J. (Water Pollut. Control Fed.)* **1980**, *52*, 310–316. .
25. Shammas, N.K.; Wang, L.K. Belt filter presses. In *Biosolids Treatment Processes*; Springer: Berlin/Heidelberg, Germany, 2007; pp. 519–539.
26. Davys, M.; Pirie, N. A belt press for separating juices from fibrous pulps. *J. Agric. Eng. Res.* **1965**, *10*, 142–145. [CrossRef]
27. Mushtaq, M. Extraction of fruit juice: An overview. *Fruit Juices* **2018**, 131–159.
28. Wakeman, R.; Tarleton, S. *Solid/Liquid Separation: Principles of Industrial Filtration*; Elsevier: Amsterdam, The Netherlands, 2005.
29. Vaxelaire, J.; Olivier, J. Compression dewatering of particulate suspensions and sludge: Effect of shear. *Dry. Technol.* **2014**, *32*, 23–29. [CrossRef]
30. Koenders, M.; Liebhart, E.; Wakeman, R. Dead-end filtration with torsional shear: Experimental findings and theoretical analysis. *Chem. Eng. Res. Des.* **2001**, *79*, 249–259. [CrossRef]
31. Hammerich, S.; Stickland, A.D.; Radel, B.; Gleiss, M.; Nirschl, H. Modified shear cell for characterization of the rheological behavior of particulate networks under compression. *Particuology* **2020**, *51*, 1–9. [CrossRef]
32. Hammerich, S. Numerische Simulation des Fest-Flüssig-Trennprozesses in Vollmantelzentrifugen: Simulationsmethode und Bestimmung des Materialverhaltens. Ph.D. Thesis, Karlsruher Institut für Technologie (KIT), Karlsruhe, Germany, 2020.
33. Bickert, G.; Vince, A. Improving Vacuum Filtration by Chemical and Mechanical Means. In Proceedings of the Thirteenth Australian Coal Preparation Conference, Mackay, Australia, 12–17 September 2010.
34. Höfgen, E.; Collini, D.; Batterham, R.J.; Scales, P.J.; Stickland, A.D. High pressure dewatering rolls: Comparison of a novel prototype to existing industrial technology. *Chem. Eng. Sci.* **2019**, *205*, 106–120. [CrossRef]
35. Massarsch, K.R. Effects of vibratory compaction. In Proceedings of the International Conference on Vibratory Pile Driving and Deep Soil Compaction, Louvain-la-Neuve, Belgium, 9–10 September 2002; Balkema: Lisse, The Netherlands, 2002; pp. 33–42.

36. Nicolas, M.; Duru, P.; Pouliquen, O. Compaction of a granular material under cyclic shear. *Eur. Phys. J. E* **2000**, *3*, 309–314. [CrossRef]
37. Roberts, A.W. Vibration of Fine Powders and Its Application. In *Handbook of Powder Science & Technology*; Fayed, M.E., Otten, L., Eds.; Springer US: Boston, MA, USA, 1997; pp. 146–201.
38. Gomaa, H.; Rao, S.; Al-Taweel, A. Intensification of membrane microfiltration using oscillatory motion. *Sep. Purif. Technol.* **2011**, *78*, 336–344. [CrossRef]
39. Ullah, A.; Shahzada, K.; Khan, S.W.; Starov, V. Purification of produced water using oscillatory membrane filtration. *Desalination* **2020**, *491*, 114428. [CrossRef]
40. Pearce, K.W. Increasing liquid expression by applying low frequency vibration. *Dry. Technol.* **1988**, *6*, 515–533. [CrossRef]
41. Guo, F.; Guo, Y.; Zhang, Y.; Liu, H.; Li, J.; Li, P.; Wu, J. Dewatering mechanism of gasification fine slag by coupled mechanical force fields and its potential guidance for efficient dewatering process. *Fuel Process. Technol.* **2020**, *205*, 106459. [CrossRef]
42. Whatnall, O.; Barber, K.; Robinson, P. Tailings Filtration Using Viper Filtration Technology—A Case Study. *Min. Metall. Explor.* **2021**, *38*, 1297–1303. [CrossRef]
43. Illies, S.; Pfinder, J.; Anlauf, H.; Nirschl, H. Filter cake compaction by oscillatory shear. *Dry. Technol.* **2017**, *35*, 66–75. [CrossRef]
44. Illies, S. Darstellungen zur Entfeuchtung von zu Rissbildung Neigenden Filterkuchen. Ph.D. Thesis, Karlsruher Institut für Technologie (KIT), Karlsruhe, Germany, 2017.
45. Yildiz, T.; Klein, S.; Gleiß, M.; Nirschl, H. Vibration compaction of compressible filter cakes for mechanical deliquoring on a horizontal vacuum belt filter. *Dry. Technol.* **2022**. [CrossRef]
46. Nirschl, H. Einfluss der Physikochemie auf die Abtrennung nanoskaliger Partikel aus Flüssigkeiten. *Chem. Ing. Tech.* **2007**, *79*, 1797–1807. [CrossRef]
47. Tiller, F.M.; Yeh, C.S.; Leu, W.F. Compressibility of paniculate structures in relation to thickening, filtration, and expression—A review. *Sep. Sci. Technol.* **1987**, *22*, 1037–1063. [CrossRef]
48. Reichmann, B.; Tomas, J. Expression behaviour of fine particle suspensions and the consolidated cake strength. *Powder Technol.* **2001**, *121*, 182–189. [CrossRef]
49. Ozcan, O.; Ruhland, M.; Stahl, W. Shear strength of mineral filter cakes. In *Studies in Surface Science and Catalysis*; Elsevier: Amsterdam, The Netherlands, 2000; Volume 128, pp. 573–585.
50. Ozcan, O.; Gonul, B.; Bulutcu, A.; Manav, H. Correlations between the shear strength of mineral filter cakes and particle size and surface tension. *Colloids Surfaces A Physicochem. Eng. Asp.* **2001**, *187*, 405–413. [CrossRef]
51. Yu, A.B.; Zou, R.P.; Standish, N. Packing of ternary mixtures of nonspherical particles. *J. Am. Ceram. Soc.* **1992**, *75*, 2765–2772. [CrossRef]
52. Anlauf, H.; Sorrentino, J.A. The influence of particle collective characteristics on cake filtration results. *Chem. Eng. Technol. Ind. Chem.-Plant Equip.-Process Eng.-Biotechnol.* **2004**, *27*, 1080–1084. [CrossRef]